Am J Transl Res 2019;11(12):7471-7478
www.ajtr.org /ISSN:1943-8141/AJTR0096747

Original Article

Evaluation of PD-1 blockade using a multicellular tumor spheroid model

Shujuan Zhou[1*], Mei Zhu[1,2,3*], Fanyan Meng[1], Jie Shao[1], Qiuping Xu[1], Jia Wei[1], Baorui Liu[1]

[1]The Comprehensive Cancer Centre of Drum Tower Hospital, Medical School of Nanjing University & Clinical Cancer Institute of Nanjing University, Nanjing, China; [2]The Comprehensive Cancer Centre, Nanjing Drum Tower Hospital Clinical College of Nanjing Medical University, Nanjing, China; [3]Department of Oncology, Xuzhou Cancer Hospital, Jiangsu, China. [*]Equal contributors.

Received May 9, 2019; Accepted November 9, 2019; Epub December 15, 2019; Published December 30, 2019

Abstract: Three-dimensional multicellular tumor spheroids are invaluable due to their ability to recapitulate major physiological characteristics of solid tumors. The lack of appropriate *in vitro* models to evaluate the effects of PD-1 blockade has restricted use of PD-1 inhibitors. Here, we established spheroids from a human gastric cell line to evaluate the cytotoxicity of the PD-1 blockade. Mature spheroids were formed 72 h after seeding tumor cells into ultra-low attachment microplates. We induced PD-L1 expression of spheroids using IFN-γ and TNF-α. Confocal images showed that PD-1 blockade enhanced T-cell cytotoxicity against PD-L1-expressing spheroids. Mechanistic studies revealed that PD-1 blockade increased expression of multiple chemokines. Altogether, our study demonstrates that tumor spheroids provide a novel platform to evaluate the effects of PD-1 blockade and might be further utilized to develop promising combination therapies.

Keywords: 3D tumor model, MCTSs, PD-1 blockade, combination therapy

Introduction

An important characteristic of solid tumors is their heterogeneous cellular composition that includes both cancer cells and stromal cells, such as infiltrating immune cells, endothelial cells, and extracellular matrix cells. Another defining characteristic is their complex biochemical gradient of nutrients, growth factors, oxygen, and pH. Intercellular interactions and biochemical gradients determine cell phenotypes and behaviors, and consequently, also determine treatment responses [1]. Two-dimensional (2D) flat cell cultures, the most commonly used *in vitro* models, do not accurately mimic *in vivo* cellular organization and biological microenvironment of solid tumors, making them inadequate for cancer research.

Three-dimensional (3D) *in vitro* tumor models are becoming increasingly recognized as more reliable tumor surrogates. Multicellular tumor spheroids (MCTSs) are one of the most extensively explored models [2]. MCTSs can recapitulate spatial architecture of different areas, including the proliferative outer layer, quiescent intermediate layer, and necrotic inner layer. Meanwhile, MCTSs preserve tumor cell interactions with other MCTSs and with extracellular matrix. MCTSs are also convenient and highly reproducible, furthering their appeal as a novel *in vitro* platform for preclinical study [3]. MCTSs have been broadly employed to assess drugs like chemotherapeutics and nanoparticles [4]. With the robust development of cancer immunotherapy, MCTSs are also becoming favored for evaluating cytotoxicity and penetration of immune cells, such as T cells and NK cells, as well as for exploring tumor immune escape mechanisms and screening immunotherapy agents or combinations preclinically [5-7].

Here, we introduced a 3D tumor model using ultra-low attachment 96-well plates to test the tumoricidal effect of PD-1 blockade (**Figure 1A**). With this approach, we aimed to extend the application of PD-1 blockade for use in combination therapies in future studies.

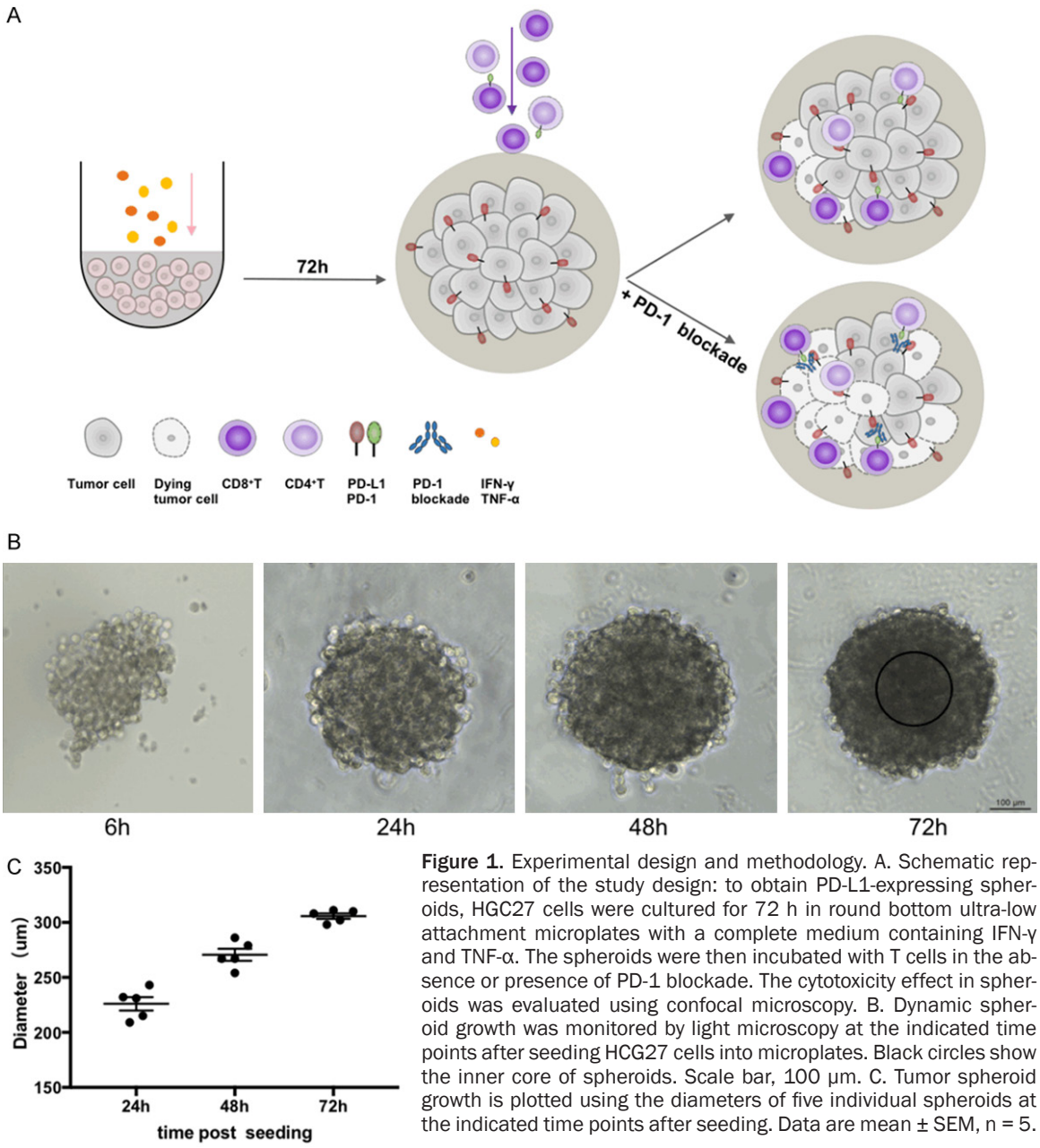

Figure 1. Experimental design and methodology. A. Schematic representation of the study design: to obtain PD-L1-expressing spheroids, HGC27 cells were cultured for 72 h in round bottom ultra-low attachment microplates with a complete medium containing IFN-γ and TNF-α. The spheroids were then incubated with T cells in the absence or presence of PD-1 blockade. The cytotoxicity effect in spheroids was evaluated using confocal microscopy. B. Dynamic spheroid growth was monitored by light microscopy at the indicated time points after seeding HCG27 cells into microplates. Black circles show the inner core of spheroids. Scale bar, 100 μm. C. Tumor spheroid growth is plotted using the diameters of five individual spheroids at the indicated time points after seeding. Data are mean ± SEM, n = 5.

Materials and methods

Cell culture

Human gastric adenocarcinoma cell line HGC-27 was purchased from the Cell Bank of Shanghai Institute of Biochemistry and Cell Biology, China, cultured in RPMI 1640 medium supplemented with 10% fetal calf serum (FCS), 100 U/ml penicillin, and 100 μg/ml streptomycin. The blood collection procedure was performed according to guidelines verified and approved by the Ethics Committee of Drum Tower Hospital. All donors signed an informed consent for scientific research statement. Peripheral blood mononuclear cells (PBMCs) were isolated from samples of healthy volunteers by centrifugation on a Ficoll density gradient and suspended in AIM-V medium (Gibco, NY, USA) containing 10% fetal bovine serum (FBS) (Gibco, NY, USA). PBMCs were cultured for 2 h for adherence. Non-adherent T lymphocytes were activated with 1,000 U/ml IFN-γ (PeproTech, NJ, USA) on day 1, 50 ng/ml OKT3 (eBioscience, CA, USA) and 300 U/ml IL-2 (Peprotech, NY, USA) on day 2. Every 2-3 days, culture medium was replaced

with fresh complete medium containing IL-2, for a total 7-10 days. All cells were incubated at 37°C and 5% CO_2, and authenticated by checking morphology by microscopy after plating at different concentrations.

Multicellular tumor spheroids

The HGC27 cells (8×10^2 in 100 μl complete media) were gently added to a 96-well clear round bottom ultra-low attachment microplate (Corning, NY, USA) and grown for 72 h to a diameter of about 300 μm. To get PD-L1-expressing spheroids, HGC27 cells were cultured in complete media containing IFN-γ (25 ng/ml) and TNF-α (20 ng/ml). MCTSs were monitored with a light microscope on day 0, 1, 2, and 3. We selected uniform and compact tumor spheroids for subsequent studies.

Flow cytometry analysis

We performed flow cytometry analysis using the following antibodies: PD-L1-PE (M1H4, BD Bioscience, CA, USA), CD3-FITC (UCHT1, BD Bioscience, CA, USA), PD-1-PE (EH12.1, BD Bioscience, CA, USA), and IgG1 isotype-PE (MOPC-21, BD Bioscience, CA, USA). All samples tested were suspended in fluorescence-activated cell sorting (FACS) buffer and stained with indicated antibodies for 30 min at 4°C in darks. Then samples were washed twice and resuspended in FACS buffer before analysis. Flow cytometry data were collected on BD Accuri C6 (BD Bioscience, CA, USA) and analyzed with FlowJo 10.4 software. For chemokines detection, PD-L1-expressing MCTSs were incubated with T cells alone (at an E:T ratio of 10:1) or T cells and PD-1 blockade (10 μg/ml) for 12 h. The supernatant fluids were harvested for chemokines quantification using BD CBA Human Chemokine Kit (BD Bioscience, NZ, USA) according to the manufacturer's instructions.

Confocal microscopy

To detect PD-L1 induction on MCTSs, spheroids were transferred to 1.5-ml Eppendorf tubes and stained with PD-L1-PE (M1H1, BD Bioscience, CA, USA) in the dark for 30 min. After washing and fixing in 4% paraformaldehyde, spheroids were subjected to ZEN 880 confocal microscopy (Zeiss, Oberkochen, Germany) and images were acquired at the mid-height of spheroids. For the cytotoxicity assay, T cells (at an E:T ratio of 10:1) or T cells with PD-1 blockade (10 μg/ml) were added to PD-L1-expressing spheroids and incubated for another 12 h. Spheroids were then stained using a viability/cytotoxicity kit (Biotium, CA, USA) in the dark for 45 min. Consecutive images slides were captured by ZEN 880 confocal microscope using the Z-stack project from the top to the middle of spheroids using 5-μm intervals. Maximum intensity projection (MIP) images were obtained in Zeiss processing software. Quantification of live and dead cell areas was performed by measuring total cell area of each dye in Image J.

Western blot analysis

HGC27 cells were cultured in complete media with or without IFN-γ/TNF-α for 72 h, collected, and then lysed with cold RIPA buffer containing protease inhibitors. Equal amounts of protein samples were subjected to sodium dodecyl sulfate-polyacrylamide gel electrophoresis (SDS-PAGE) and transferred to polyvinylidene difluoride (PVDF) membranes. Membranes were blocked with 5% bovine serum albumin (BSA) for 2 h at RT and incubated with an anti-PD-L1 antibody (ab237726, Abcam, Cambrige, UK) at 4°C overnight. Subsequently, membranes were incubated with a secondary antibody (ab97051, Abcam, Cambrige, UK) for 1-2 h at RT. Membranes were washed and examined by the enhanced chemiluminescence solution and then visualized with a ChemiDoc XRS + system (Bio-Rad, CA, USA).

Statistics

Graphpad Prism 7.0 software was used for all statistical analysis. Data are presented as mean ± SEM. The Student's *t*-test was used to determine the significances between groups and values were considered to be statistically significant if $P < 0.05$.

Results

Preparation of MCTSs

We generated tumor spheroids by seeding HGC27 cells into ultra-low attachment 96-well plates (**Figure 1B**). HGC27 cells aggregated at the round bottom of plates as a cell mass at 6 h (day 0) after seeding. At 24 h after seeding (day 1), tumor cells had self-assembled into a moderately compact spherical appearance. Cellular reorganization and proliferation increased the diameter and compactness of the ma-

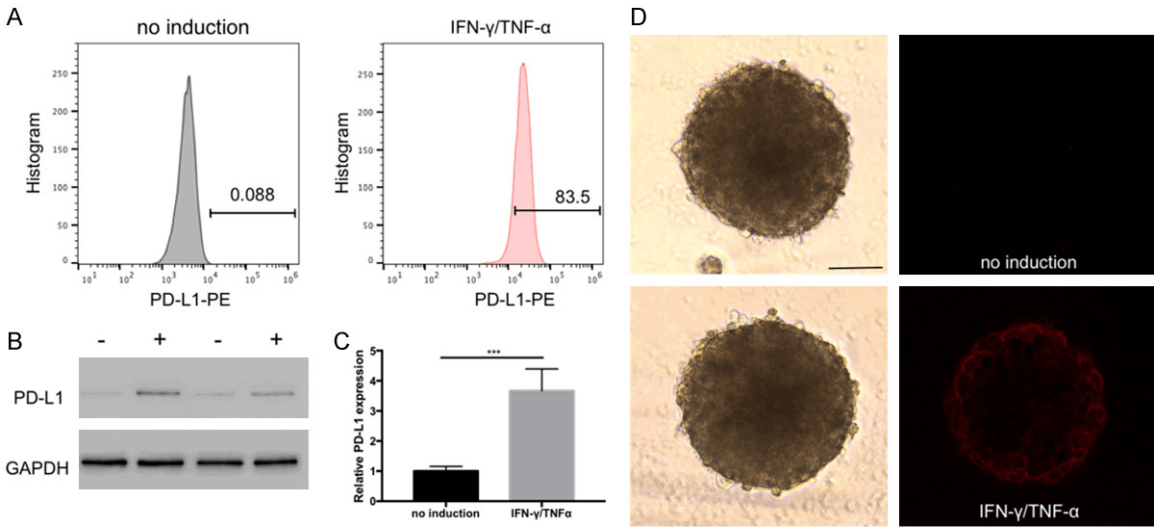

Figure 2. PD-L1 induction in HGC27 cells. HGC27 were cultured for 72 h in the absence or presence of IFN-γ/TNF-α. A. Monolayer cells were collected and then subjected to flow cytometry for PD-L1 detection. B, C. PD-L1 expression of monolayer cells was detected by western blot analysis. -, without IFN-γ/TNF-α; +, with IFN-γ/TNF-α. D. Confocal microscopy images of HGC27 MCTSs. Left panel, bright field; right panel, PE channel. PD-L1 was detected by an anti-PD-L1 antibody conjugated to PE. Scale bar, 100 μm. Data are mean ± SEM, n = 5. ***P < 0.01.

ss on day 2. On day 3, mature spheroids were of uniform size and morphology and suitable for use in further experiments (**Figure 1C**). These MCTSs had an inner core comprised of quiescent and necrotic tumor cells, and were characterized by oxygen and pH gradients similar to biological conditions of solid tumors *in vivo* [1].

Induction of PD-L1 expression in HGC27 cells and MCTSs

Then we examined PD-L1 expression in HGC27 cells and found that these cells had low expression of PD-L1 at baseline (0.088%). However, PD-L1 expression was markedly upregulated (83.5%) after induction with IFN-γ and TNF-α (**Figure 2A**), which was further validated by western blot analysis (**Figure 2B**, **2C**). We observed similar results in MCTSs. PD-L1 expression was detected on the cell membranes of HGC27 in spheroids after induction, whereas there was very low expression of PD-L1 in MCTSs without induction (**Figure 2D**).

PD-1 blockade enhanced T-cell cytotoxicity in MCTSs

The above PD-L1-high tumor spheroids were established to study the effect of PD-1 blockade on spheroid viability. PD-1 expression was found in about 10% of T cells (**Figure 3A**). We found that PD-1 blockade dramatically increased T-cell cytotoxicity, as judged by spheroid morphology, volume, and tumor cell death (**Figure 3B**). Spheroids incubated with T cells alone maintained integrity, whereas tumor spheroids in the PD-1 blockade group almost completely lost spherical shape and compactness. Spheroid destruction also resulted in smaller average diameters (183.2 μm ± 4.042 μm vs 288.2 μm ± 4.532 μm) (**Figure 3C**). Additionally, we quantified live and dead cells in an assay by visualizing tumor cell killing. In this assay, live cells were indicated by green fluorescence and dead cells by red fluorescence. We observed a limited number of dead cells in MCTSs in the group treated with only T cells. In contrast, the addition of PD-1 blockade increased the number of dead cells throughout all layers of spheroids, and decreased the number of living cells (**Figure 3D**).

PD-1 blockade upregulated expression of chemokines

PD-1 blockade can restore the antitumor activity of T cells and thus improve cytotoxicity in MCTSs [8, 9]. Given that MCTS destruction also requires T-cell migration into inner tumor cell layers, we hypothesized that PD-1 blockade might affect T-cell recruitment into MCTSs. Recent studies report that PD-1 blockade can increase the expression of chemokines, such as CXCL10 and CXCL9, within the tumor microenvironment (TME) in mouse models [10, 11]. Here, we found that expression of chemokines, including

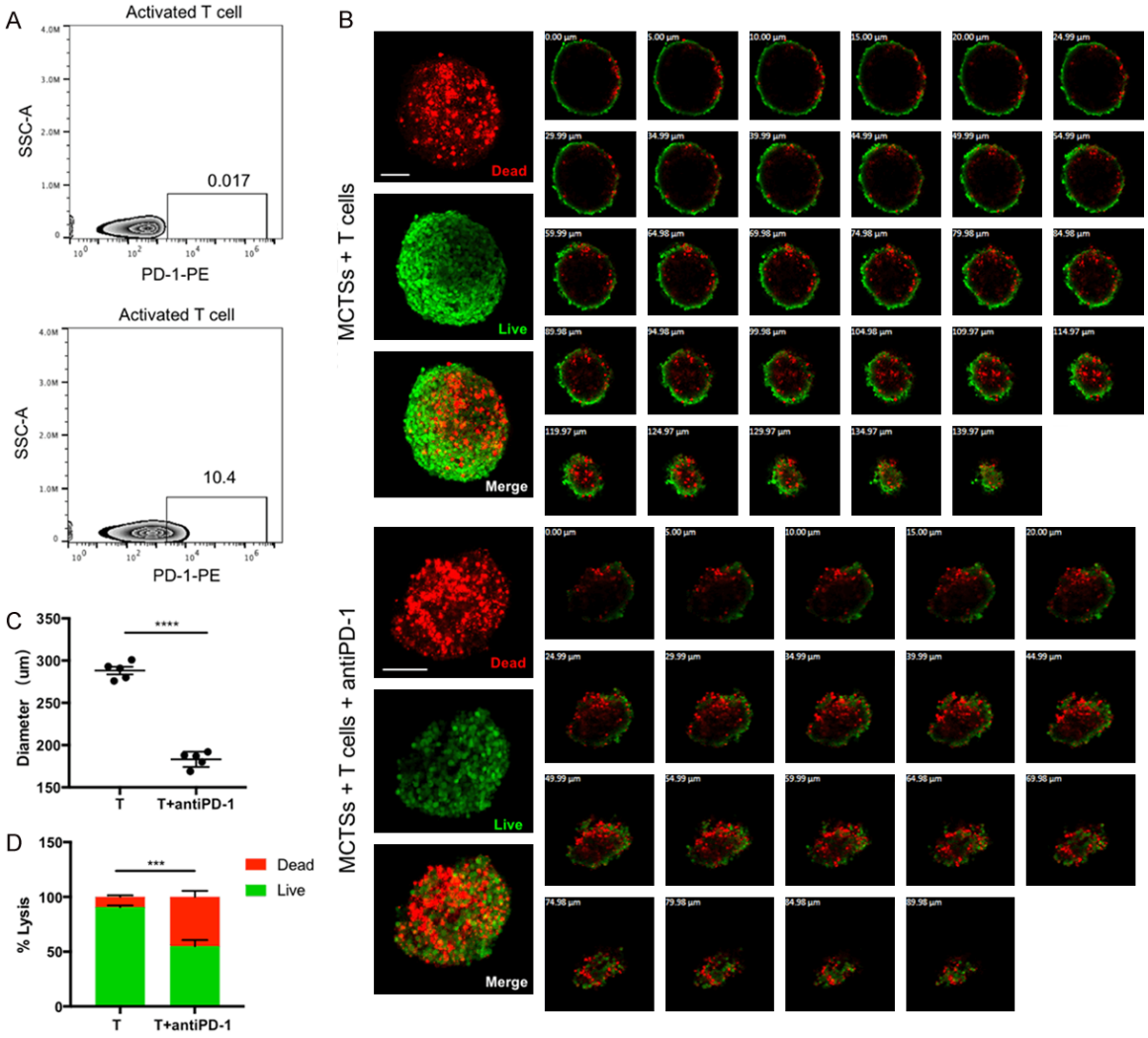

Figure 3. The effect of PD-1 blockade on T-cell cytotoxicity in MCTSs. A. PD-1 expression in activated T cells was determined by flow cytometry using a PE isotype control (upper) and PE-conjugated anti-PD-1 antibody (lower). B. Representative confocal images of MCTSs treated with T cells alone (upper panel) or T cells and PD-1 blockade (lower panel) for 12 h. The left columns of each panel show the maximum intensity projection (MIP) images of MCTSs. Dead tumor cells in MCTSs are shown by red fluorescence (EthD-1) and live tumor cells by green fluorescence (calcein AM). The right columns were consecutive slides with 5-μm intervals in a Z-stack project, scanned from the top to the middle of MCTSs. Scale bar, 50 μm. C. The diameters of MCTSs in two groups after 12 h treatment. D. The MCTSs lysis was evaluated by comparing total area of live/dead cells in MIP images. Data are shown as mean ± SEM, n = 5. ***P < 0.001, ****P < 0.0001. anti-PD-1, PD-1 blockade.

CXCL10, CXCL9, CXCL8, CCL2, and CCL5, were generally significantly upregulated in the supernatant after addition of PD-1 blockade (**Figure 4A-C**). The results suggest that chemokine induction may contribute to a novel mechanism for the tumoricidal effect of PD-1 blockade in MCTSs.

Discussion

PD-1/PD-L1 blockades are important strategies to boost cancer therapy in the immuno-oncology field. Six PD-1/PD-L1 blockades covering 14 cancer types have been approved since 2006 [12]. However, satisfactory responses to treatment using PD-1/PD-L1 blockades are only observed in a minority of patients and the resistance mechanisms against PD-1/PD-L1 blockades is not fully understood. Combination therapies of PD-1/PD-L1 blockades and other treatments are promising strategies to overcome resistance and broaden patient responses. As of September 2018, there were 1,716 combination trials for treatments that

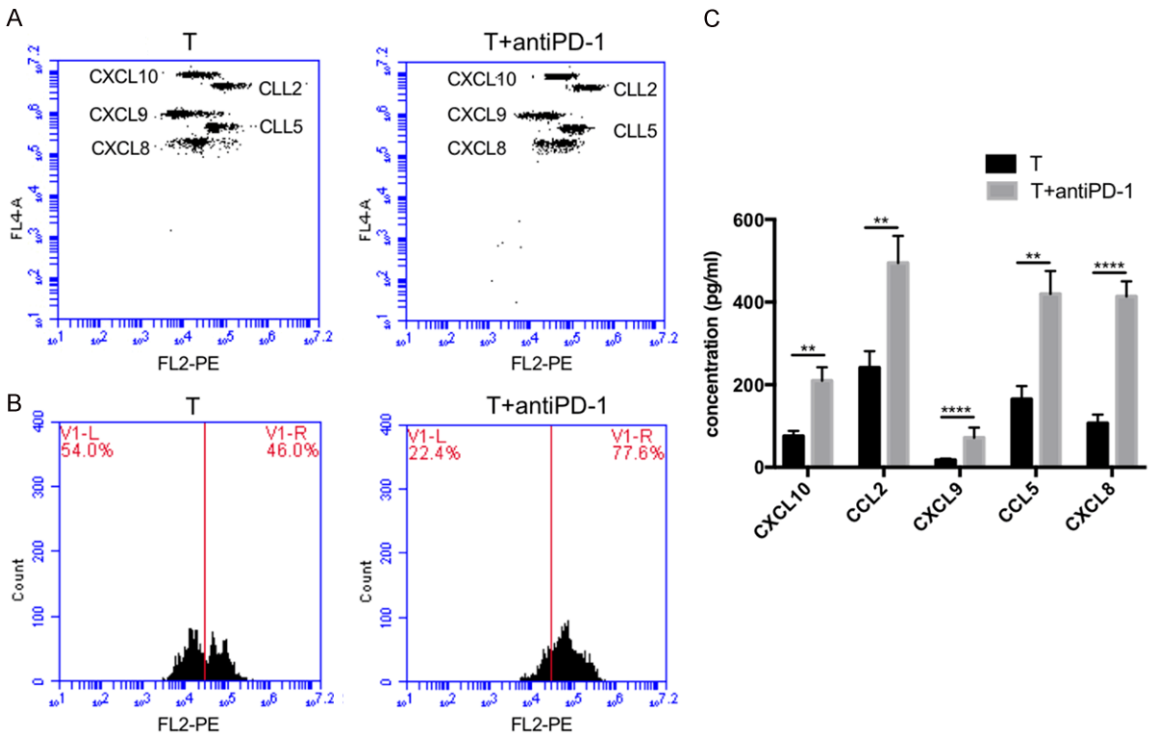

Figure 4. PD-1 blockade induced expression of chemokines in supernatant collected from co-culture of T cells and MCTSs. A. Flow cytometry results showing level of different chemokines without (left) or with (right) PD-1 blockade. The five clusters indicate CXCL10, CCL2, CXCL9, CCL5, and CXCL8 from top to bottom. Expression level of each chemokine is indicated by their PE fluorescence intensity. B. Total PE fluorescence intensity of five chemokines without (left) or with (right) PD-1 blockade. C. Quantification and analysis of chemokine levels in two groups. Data are mean ± SEM, n = 3. **P < 0.01, ****P < 0.0001. anti-PD-1, PD-1 blockade.

included PD-1/PD-L1 blockades [13]. Novel *in vitro* tumor models may accelerate the identification of resistance mechanisms and facilitate the development of effective combination therapies. In this study, we described an approach for rapid and functional assessment of PD-1 blockade using PD-L1-induced tumor spheroids. MCTSs could be easily obtained 72 h after seeding tumor cells into ultra-low attachment plates, and PD-L1 expression in MCTSs increased after stimulation by IFN-γ and TNF-α. Confocal images of spheroids with live/dead cell staining revealed the killing capacity of PD-1 blockade. The MCTSs model could be widely utilized to preclinically evaluate combination therapies *in vitro*, providing rationale to guide prioritization of combination strategies that could be translated to the clinic.

Compared with 2D cell cultures, spheroids can simulate *in vivo* solid tumors more precisely because of their three-dimensional structure and ability to maintain tumor cell interactions with other spheroids and ECM secretions. Biomedical gradients for nutrients and oxygen may also be recapitulated in spheroids with a diameter > 200 μm [14]. Unlike other 3D tumor models, including organoid cultures from stem cells and patient-derived xenografts (PDXs), MCTSs formation is quickly and easily performed, taking only 2-3 days to generate mature spheroids [15]. Recently, some researchers have demonstrated that MCTSs primarily comprise of cultured tumor cells and lack diverse stromal and immune components within the TME [16]. Given these findings, the researchers recommended murine-and patient-derived organotypic tumor spheroids as *ex vivo* systems to evaluate PD-1 blockade, as these models retained lymphoid and myeloid immune cell populations and cytokine secretion profiles of the TME. Sensitivity and resistance to PD-1 blockade *in vivo* was successfully recapitulated in these models [16-18]. However, inconsistencies between the murine and human immune systems, the complexity of obtaining patient-derived tumor specimens, and the unique requirements for microfluidic culture conditions, are limitations to using organotypic tumor spheroids in drug assessment. In comparison,

MCTS models have advantages in speed and convenience. Moreover, advanced MCTSs have been developed to better emulate the *in vivo* TME by co-culture with immune cells, fibroblasts, and endothelial cells [19].

In summary, this study presents a novel *in vitro* 3D model using human tumor cell lines to evaluate response to PD-1 blockade. Future studies may extend this model to facilitate preclinical development of effective combination therapies and drive translational research efforts toward clinical application.

Acknowledgements

This study was funded by The National Key Research and Development Program of China (No. 2017YFC1308900), National Natural Science Foundation of China (No. 81872146, 8167-2367), The National Major Projects for "Major New Drugs Innovation and Development" (No. 2018ZX09301048-003), and Nanjing Medical Science and Technique Development Foundation (No. QRX17038).

Disclosure of conflict of interest

None.

Address correspondence to: Dr. Baorui Liu, The Comprehensive Cancer Centre of Drum Tower Hospital, Medical School of Nanjing University, Clinical Cancer Institute of Nanjing University, 321 Zhongshan Road, Nanjing 210008, China. Tel: +86-25-83107081; Tax: +86-25-83317016; E-mail: baoruiliu@nju.edu.cn

References

[1] Baker BM and Chen CS. Deconstructing the third dimension - how 3D culture microenvironments alter cellular cues. J Cell Sci 2012; 125: 3015-3024.

[2] Ferreira LP, Gaspar VM and Mano JF. Design of spherically structured 3D in vitro tumor models-Advances and prospects. Acta Biomater 2018; 75: 11-34.

[3] Zanoni M, Pignatta S, Arienti C, Bonafe M and Tesei A. Anticancer drug discovery using multicellular tumor spheroid models. Expert Opin Drug Discov 2019; 14: 289-301.

[4] Huang BW and Gao JQ. Application of 3D cultured multicellular spheroid tumor models in tumor-targeted drug delivery system research. J Control Release 2018; 270: 246-259.

[5] Hirt C, Papadimitropoulos A, Mele V, Muraro MG, Mengus C, Iezzi G, Terracciano L, Martin I and Spagnoli GC. "In vitro" 3D models of tumor-immune system interaction. Adv Drug Deliv Rev 2014; 79-80: 145-154.

[6] Giannattasio A, Weil S, Kloess S, Ansari N, Stelzer EH, Cerwenka A, Steinle A, Koehl U and Koch J. Cytotoxicity and infiltration of human NK cells in in vivo-like tumor spheroids. BMC Cancer 2015; 15: 351.

[7] Sherman H, Gitschier HJ and Rossi AE. A novel three-dimensional immune oncology model for high-throughput testing of tumoricidal activity. Front Immunol 2018; 9: 857.

[8] Topalian S, Drake C and Pardoll D. Immune checkpoint blockade: a common denominator approach to cancer therapy. Cancer Cell 2015; 27: 450-61.

[9] Chang CH, Wang Y, Li RX, Rossi DL, Liu DL, Rossi EA, Cardillo TM and Goldenberg DM. Combination therapy with bispecific antibodies and PD-1 blockade enhances the antitumor potency of T cells. Cancer Res 2017; 77: 5384-5394.

[10] Chheda ZS, Sharma RK, Jala VR, Luster AD and Haribabu B. Chemoattractant receptors BLT1 and CXCR3 regulate antitumor immunity by facilitating CD8+ T cell migration into tumors. J Immunol 2016; 197: 2016-2026.

[11] Weiyi P, Chengwen L, Chunyu X, Yanyan L, Jieqing C, Yan Y, Hideo Y, Overwijk WW, Gregory L and Laszlo R. PD-1 blockade enhances T-cell migration to tumors by elevating IFN-γ inducible chemokines. Cancer Res 2012; 72: 5209-5218.

[12] Mellman I, Coukos G and Dranoff G. Cancer immunotherapy comes of age. Nature 2011; 480: 480-489.

[13] Tang J, Yu JX and Lin YQ. The clinical trial landscape for PD1/PDL1 immune checkpoint inhibitors. Nat Rev Drug Discov 2018; 17: 854-854.

[14] Khaitan D, Chandna S, Arya MB and Dwarakanath BS. Establishment and characterization of multicellular spheroids from a human glioma cell line; Implications for tumor therapy. J Transl Med 2006; 4: 12.

[15] Gao D, Vela I, Sboner A, Iaquinta PJ, Karthaus WR, Gopalan A, Dowling C, Wanjala JN, Undvall EA, Arora VK, Wongvipat J, Kossai M, Ramazanoglu S, Barboza LP, Di W, Cao Z, Zhang QF, Sirota I, Ran L, MacDonald TY, Beltran H, Mosquera JM, Touijer KA, Scardino PT, Laudone VP, Curtis KR, Rathkopf DE, Morris MJ, Danila DC, Slovin SF, Solomon SB, Eastham JA, Chi P, Carver B, Rubin MA, Scher HI, Clevers H, Sawyers CL and Chen Y. Organoid cultures derived from patients with advanced prostate cancer. Cell 2014; 159: 176-187.

[16] Jenkins RW, Aref AR, Lizotte PH, Ivanova E, Stinson S, Zhou CW, Bowden M, Deng JH, Liu HY, Miao DN, He MX, Walker W, Zhang G, Tian

T, Cheng CR, Wei Z, Palakurthi S, Bittinger M, Vitzthum H, Kim JW, Merlino A, Quinn M, Venkataramani C, Kaplan JA, Portell A, Gokhale PC, Phillips B, Smart A, Rotem A, Jones RE, Keogh L, Anguiano M, Stapleton L, Jia ZH, Barzily-Rokni M, Canadas I, Thai TC, Hammond MR, Vlahos R, Wang ES, Zhang H, Li S, Hanna GJ, Huang W, Hoang MP, Piris A, Eliane JP, Stemmer-Rachamimov AO, Cameron L, Su MJ, Shah P, Izar B, Thakuria M, LeBoeuf NR, Rabinowits G, Gunda V, Parangi S, Cleary JM, Miller BC, Kitajima S, Thummalapalli R, Miao BC, Barbie TU, Sivathanu V, Wong JH, Richards WG, Bueno R, Yoon CH, Miret J, Herlyn M, Garraway LA, Van Allen EM, Freeman GJ, Kirschmeier PT, Lorch JH, Ott PA, Hodi FS, Flaherty KT, Kamm RD, Boland GM, Wong KK, Dornan D, Paweletz CP and Barbie DA. Ex Vivo profiling of PD-1 blockade using organotypic tumor spheroids. Cancer Discov 2018; 8: 196-215.

[17] Balko JM and Sosman JA. A critical need for better cancer immunotherapy models: are organotypic tumor spheroid cultures the answer? Cancer Discov 2018; 8: 143-145.

[18] Deng J, Wang ES, Jenkins RW, Li S, Dries R, Yates K, Chhabra S, Huang W, Liu H and Aref AR. CDK4/6 inhibition augments anti-tumor immunity by enhancing T cell activation. Cancer Discov 2017; 8: CD-17-0915.

[19] Lamichhane SP, Arya N, Kohler E, Xiang S, Christensen J and Shastri VP. Recapitulating epithelial tumor microenvironment in vitro using three dimensional tri-culture of human epithelial, endothelial, and mesenchymal cells. BMC Cancer 2016; 16: 581.